

Edge Detection Through Integrated Morphological Gradient and Type 2 Fuzzy Systems

^[1]Priyanka Thakur ^[2]Dr.Arshia Azam

^[1]Assistant Professor, ^[2]Professor

^{[1][2]}Department of Electronics and Communication

^[1]VIF College of Engineering and Technology

^[2]Maulana Azad National Urdu University

^{[1][2]}Hyderabad, India

^[1]priyanka.thkr25@gmail.com, ^[2]aazam_04@yahoo.co.in

Abstract—We present, in this paper, effective edge detection methods using type 2 fuzzy inference systems which are known for their uncertainty handling ability. These methods are clubbed up with morphological gradient to enhance their edge detection capabilities. We emphasize on the application of generalized type 2 fuzzy system to the image and detection of edge. We then compare the Morphological Gradient with the type 1 fuzzy system, integrated interval type 2 fuzzy system (Interval type 2 fuzzy logic applied upon Morphological Gradient Technique) and generalized type 2 fuzzy system (Generalized type 2 fuzzy logic applied upon Morphological Gradient Technique). Also these edge detectors are tested on images added with 0.001 white gaussian noise and salt and pepper noise. Recall, precision and PFOM are also calculated for each system and compared.

Keywords—Morphological Gradient, Sobel, Laplacian of Gaussian, Fuzzy Logic, Mamdani, Fuzzification, Type Reduction, Defuzzification.

I. INTRODUCTION

An edge may be the result of changes in light absorption, its shade, texture and color, and these changes can be used to determine the depth, size, positioning, alignment and surface properties of a digital image. An edge is not only the boundary between an object and the background, but also the boundary between overlapping objects. In analyzing the image digitally, edge detection involves filtering extraneous and immaterial information to select the edge points. The detection of minute changes, which may be mixed up by noise, depends on the pixel threshold of change that defines an edge. Detection of such continuous edges is very strenuous and time consuming especially when an image is corrupted by noise[1].

Edge detection of an image reduces significantly the amount of data and filters out information that may be regarded as irrelevant, preserving the important structural properties of an image[2]. Therefore, edges detected from the original image contain major information, which can be stored in very less space than the original image. The main goal of the vision systems based on computational intelligence techniques is to achieve better edge detection when image processing is performed under high noise levels

The main application areas of edge detection include geography, military, medicine, robotics,

meteorology and pattern recognition systems[3][4][5][6]. The paper is organized as follows. The integrated fuzzy system is described in section II and the simulations and results are shown in section III. Section IV and V give the conclusion and future scope respectively.

II. FUZZY LOGIC APPROACH

Various edge detection methods have been developed in the process of finding the perfect edge detector. Most of these can be categorized as gradient based and laplacian based edge detectors[7]. In this paper, a type 1 fuzzy system and two type 2 fuzzy systems are implemented.

The first step in the process is determining if the image is a color image and converting it into a grayscale image for the sake of simplified analysis. To this extracted grayscale edge map, we apply the morphological gradient.

A. Morphological Gradient

The morphological gradient can be defined as the difference between intensity values of two neighboring pixels that belong to a given structural element, for a gray scale image. A classic definition of morphological gradient is given in (1)

$$\nabla(f) = \delta_g(f) - \varepsilon_g(f) \quad (1)$$

We use D instead of $\nabla(f)$. The coefficients z_i are calculated as shown in Fig. 1 and Fig. 2 shows the directions in which the difference in intensity values are calculated using eq 2. The edge S, for one pixel, is calculated with eq 3 by summing up the difference of intensity values calculated in all 4 directions for that pixel[8].

$$D1 = \sqrt{(z_5 - z_2)^2 + (z_5 - z_8)^2} \quad (2a)$$

$$D2 = \sqrt{(z_5 - z_4)^2 + (z_5 - z_6)^2} \quad (2b)$$

$$D3 = \sqrt{(z_5 - z_1)^2 + (z_5 - z_9)^2} \quad (2c)$$

$$D4 = \sqrt{(z_5 - z_3)^2 + (z_5 - z_7)^2} \quad (2d)$$

$$S = D1 + D2 + D3 + D4 \quad (3)$$

$z_1 = f(x-1, y-1)$	$z_3 = f(x+1, y-1)$	$z_3 = f(x+1, y-1)$
$z_4 = f(x+1, y)$	$z_5 = f(x, y)$	$z_6 = f(x+1, y)$
$z_7 = f(x-1, y+1)$	$z_8 = f(x, y+1)$	$z_9 = f(x, y+1)$

Figure 1 3x3 matrix indicating the coefficients Z_i .

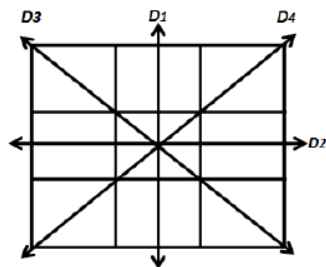


Figure 2 3x3 matrix indicating the directions D_i

B. Fuzzy Inference System

The basic difference between integrated type 2 fuzzy system (IT2FS) and generalized type 2 fuzzy system (GT2FS) is that for each value, the membership degree at each point in the uncertain range is 1 or equal in IT2FS and different in GT2FS [9][10]. It is depicted in Fig 3, 4 respectively.

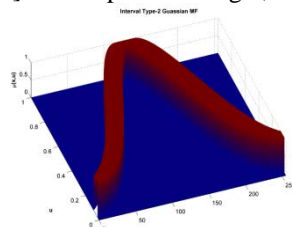


Figure 3 Interval type 2 membership function

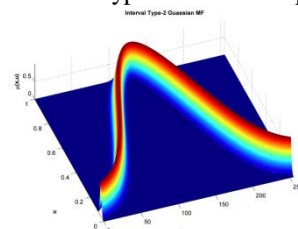


Figure 4 Generalized type 2 membership function

The outputs D_i of the morphological gradient, are given as the inputs to the generalized type 2 fuzzy inference system. The basic block diagram of fuzzy inference system is shown in Fig 5. The crisp inputs are fuzzified using the fuzzification process where the fuzzy sets are created based on the

gray scale value of images and membership functions are assigned [11]. The membership functions are shown in figure (4). Gaussian membership functions are used in the entire approach.

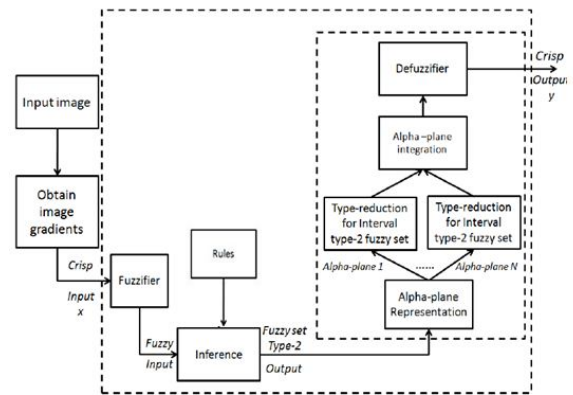


Figure 5 Block diagram of generalized type 2 fuzzy inference system.

$$low_i = \min(D_i) \quad (4)$$

$$high_i = \max(D_i) \quad (5)$$

$$medium_i = low_i + (high_i - low_i)/2 \quad (6)$$

$$\sigma_i = high_i / 5 \quad (7)$$

$$edge_i = 1 \quad (8)$$

$$no_edge_i = 0 \quad (9)$$

$$\sigma_i = edge_i / 4 \quad (10)$$

$$m_1 = high_i, m_2 = m_1 + FOU \quad (11)$$

$$\tilde{\mu}(x) = [\underline{\mu}(x), \bar{\mu}(x)] = igaussmtype2(x, [\sigma_x, m_1, m_2]) \quad (12)$$

$$m_x = \frac{m_1 + (m_1 * FOU) + high_i}{2} \quad (13)$$

$$m_x = \frac{m_2 + m_1}{2} \quad (14)$$

$$\sigma_u = \frac{\delta}{2\sqrt{6}} + \epsilon \quad (15)$$

$$p_x = gaussmf(x, [\sigma_x, m_x]) = \exp\left[-\frac{1}{2}\left(\frac{x-m_x}{\sigma_x}\right)^2\right] \quad (16)$$

$$\tilde{\mu}(x, u) = gaussmf(u, [\sigma_u, p_x]) = \exp\left[-\frac{1}{2}\left(\frac{x-p_x}{\sigma_u}\right)^2\right] \quad (17)$$

The Gaussian membership functions for each D input are obtained using eq (12)–(17), and the means of each function are obtained with eq (11) and the σ value is obtained with (7). The inference system has one output S (the edge), the linguistic values used for the output are: *edge* and *no_edge*, and we selected the range $[0, 1]$, since the input image was normalized in this range, where the minimum value for the output is represented by (9) and maximum by (8). The Footprint of uncertainty (FOU), is assumed a random value between 0 and 1. In Fig. 6, we show

the linguistic variables with generalized type-2 membership functions.

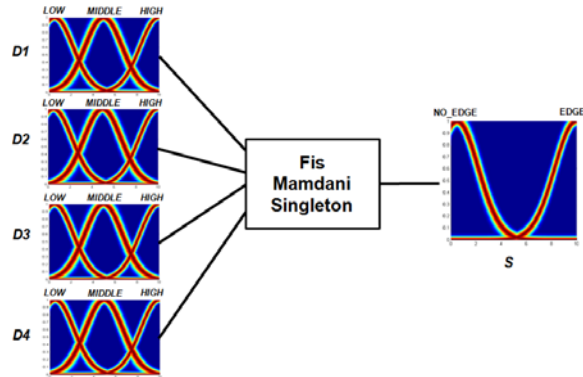


Figure 6 Generalized type 2 fuzzy membership functions for input and output.

Next, we use 3 rules that help describe the existing relationship between the image gradients. The fuzzy rules are the following.

- a) If (D1 is HIGH) or (D2 is HIGH) or (D3 is HIGH) or (D4 is HIGH) then (S is EDGE)
- b) If (D1 is MEDIUM) or (D2 is MEDIUM) or (D3 is MEDIUM) or (D4 is MEDIUM) then (S is EDGE)
- c) If (D1 is LOW) and (D2 is LOW) and (D3 is LOW) and (D4 is LOW) then (S is NO_EDGE).

Next, to perform inference, the theory of alpha planes was used and performed using (18).

$$\tilde{A}\alpha = \{(x, u), \mu_{\tilde{A}}(x, u) \geq \alpha | \forall x \in X, \forall u \in J_X \subseteq [0, 1]\}$$

$$= \int_{\forall x \in X} \int_{\forall u \in J_X} \{(x, u) | f_x(u) \geq \alpha\} \quad (18)$$

To carry out the defuzzification process, the heights method of type reduction was used [12][13]. This method replaces each rule output set by a singleton that is the maximum point of the membership function in the output, and after that calculates the centroid of the type-1 set by using these singletons [14][15]. The output of the heights defuzzification is given by (19)

$$h(x) = \frac{\sum_{l=1}^M l \mu_B^l(l)}{\sum_{l=1}^M \mu_B^l(l)} \quad (19)$$

The type reduction was performed applying the theory of Karnik and Mendel, and this reduction is given by (20)(21)[16][17]

$$y_l = \frac{\sum_{i=1}^L f^{-i}(x')h^i + \sum_{j=L+1}^M f^j(x')h^j}{\sum_{i=1}^L f^{-i}(x') + \sum_{j=L+1}^M f^j(x')} \quad (20)$$

$$y_r = \frac{\sum_{i=1}^R f^i(x')h^i + \sum_{i=R+1}^M f^{-i}(x')h^i}{\sum_{i=1}^R f^i(x') + \sum_{i=R+1}^M f^{-i}(x')} \quad (21)$$

The results of alpha planes are integrated by (22)(23)[18][19],

$$\hat{Y}_j^r(x') = \frac{\sum_{i=1}^N \alpha_i \alpha_i \hat{y}_j^r(x')}{\sum_{i=1}^N \alpha_i} \quad (22)$$

$$\hat{Y}_j^l(x') = \frac{\sum_{i=1}^N \alpha_i \alpha_i \hat{y}_j^l(x')}{\sum_{i=1}^N \alpha_i} \quad (23)$$

After realizing the type reduction and integrating the results of all alpha planes, defuzzification was performed by using the average of y_l and y_r , to obtain the defuzzified output of a generalized singleton type-2 FLS (24) [18] and the final edge map is obtained..

$$\hat{Y}_j(x') = \frac{\hat{Y}_j^l(x') + \hat{Y}_j^r(x')}{2} \quad (24)$$

III. SIMULATION RESULTS

The simulation results of the edge detectors implemented in MATLABR2010a software [20] are shown. This simulation is done on the test image lena and two synthetic images, square and polar shown in figure 11[21], created in MATLABR2010a. The results of Morphological gradient, Integrated Type 1 fuzzy logic system and Integrated interval T2FS and integrated generalized T2FS are shown in fig 7, 8, 9, 10 respectively..

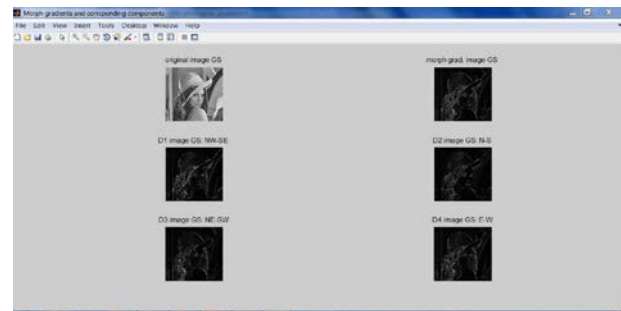


Figure 7 Simulation result of the morphological gradient with the test image lena.

In the simulation results, MG+T1FS indicates integrated morphological gradient and Type 1 fuzzy system. Similarly, MG+IT2FS represents integrated morphological gradient and integrated type 2 fuzzy system and MG+GT2FS denotes integrated morphological gradient and generalized type 2 fuzzy system.

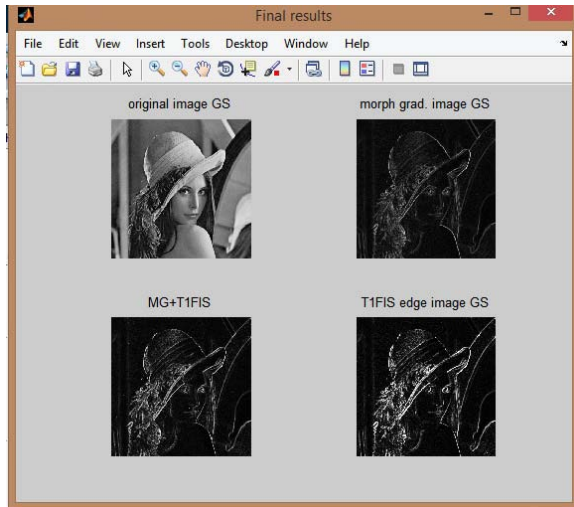


Figure 8 Simulation result of T1FIS and integrated T1FIS.

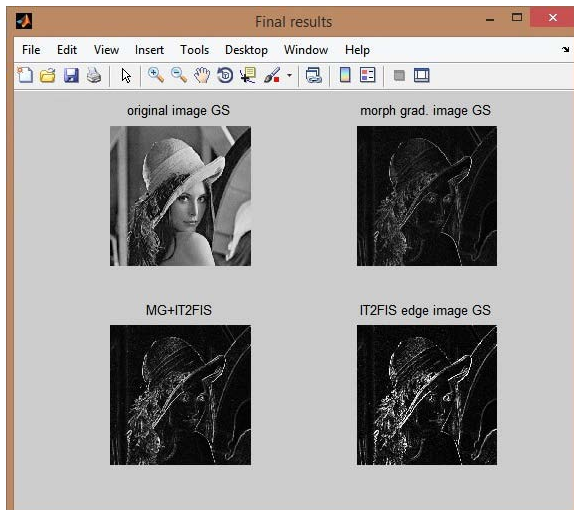


Figure 9 Simulation result of IT2FIS and Integrated IT2FIS.

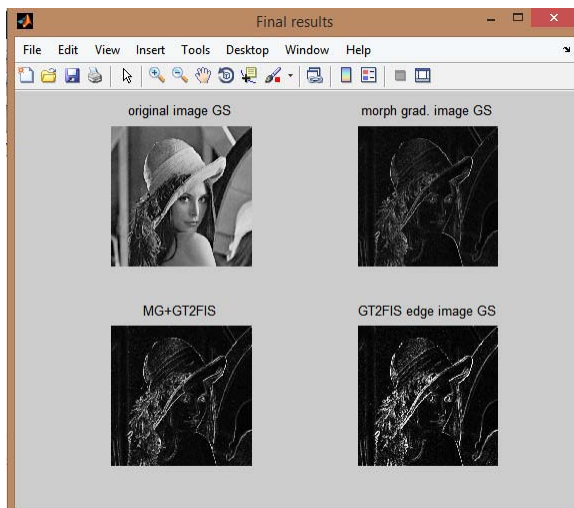


Figure 10 Simulation result of GT2FIS and Integrated GT2FIS.

The Pratts Figure of Merit is calculated on the synthetic images and the values are shown in Table 1. The Peak Signal to Noise Ratio values of these edge detectors with the synthetic images in noiseless conditions, with 0.001 white Gaussian noise and salt and pepper noise are tabulated in Table 2, while precision and recall values are shown in Table 3.



Figure 11 Square and Polar Synthetic Image

Table 1 PFOM values for noiseless synthetic images

Edge Detector Used	Type of Image	Pratts Figure of Merit
MG +T1FIS	Square	0.8935
	Polar	0.8669
MG + IT2FIS	Square	0.9264
	Polar	0.9177
MG + GT2FIS	Square	0.9233
	Polar	0.9134

Table 2 PSNR values for noiseless and noisy synthetic images.

Edge Detector Used	Type of Image	PSNR (in dB)		
		Noiseless	Salt and Pepper noise	0.001 Gaussian noise
MG +T1FIS	Square	12.9071	9.8923	11.5839
	Polar	12.5996	8.4562	10.7294
MG +IT2FIS	Square	12.2094	10.9246	11.9045
	Polar	13.1846	10.4479	12.7368
MG +GT2FIS	Square	13.8984	11.9386	13.3372
	Polar	13.4434	11.3788	12.9173

Table 3 Precision and Recall values of the implemented edge detectors.

Parameter	MG + T1FIS	MG + IT2FIS	MG + GT2FIS
Precision	0.600216	0.600218	0.600398
Recall	0.992896	0.992892	0.992653

It can be noted that, regardless of the presence of noise, integrated GT2FS gives the maximum performance in terms of PSNR and Recall. Integrated IT2FS gives highest PFOM value while, Precision value is the highest for integrated TIFS.

IV. CONCLUSION

The edge detectors with integrated morphological gradient and type 2 systems are implemented. All the fuzzy systems are found to be working very well with reference to at least one of the parameters. But, it is to be noted that their performance might vary with the image it is tested upon.

V. FUTURE ENHANCEMENTS.

These integrated fuzzy logic techniques can be further implemented on videos and probably extended for uses in motion detection etc. It can also be tested on various other types of corrupt images affected with shot noise, quantization noise etc.

REFERENCES

- [1] V. Torre, T. A. Poggio, On Edge Detection, *IEEE Transactions on Pattern Analysis and Machine Intelligence*, vol. 8, no. 6., pp. 147–163, 1986.
- [2] J. F. Canny. “A computational approach to edge detection”. *IEEE Trans. Pattern Anal. Machine Intell.*, vol. PAMI-8, no. 6, pp. 679-697, 1986
- [3] T. Shimada, F. Sakaida, H. Kawamura, and T. Okumura, “Application of an edge detection method to satellite images for distinguishing sea surface temperature fronts near the Japanese coast,” *Remote Sensing of Environment*, vol. 98, no. 1, pp. 21–34, 2005.
- [4] A. A. Goshtasby, 2-D and 3-D Image Registration: for Medical, Remote Sensing, and Industrial Applications, pp. 34–39. 2005.
- [5] A. . Kazerooni, A. Ahmadian, N. D. Serej, H. S. Rad, H. Saberi, H. Yousefi, and P. Farnia, “Segmentation of brain tumors in MRI images using multi-scale gradient vector flow,” in *Engineering in Medicine and Biology Society, EMBC, 2011 Annual International Conference of the IEEE*, pp. 7973–7976, 2011.
- [6] B. Siliciano, L. Sciavicco, L. Villani, and G. Oriolo, *Robotics: Modelling, Planning and Control*, pp. 415– 418, 2010.
- [7] Raman Maini, Dr. Himanshu Aggarwal, Study and Comparison of Various Image Edge Detection Techniques, *International Journal of Image Processing (IJIP)*, Volume (3) : Issue (1), ISSN - 1985-2304. Pp. 1-11, 2009.
- [8] Y. Becerikli and T. M. Karan, “A New Fuzzy Approach for Edge Detection of Image Edges,” *Computational intelligence and bioinspired systems*. Berlin: LNCS, Springer Verlag., pp. 943–951, 2005.
- [9] C. Wagner and H. Hagra, “Towards general type-2 fuzzy logic systems based on zSlices,” *Fuzzy Systems, IEEE Transactions on*, vol. 18, no. 4, pp. 637–660, 2010.
- [10] J. M. Mendel and R. I. B. John, “Type-2 fuzzy sets made simple,” *IEEE Transactions on Fuzzy Systems*, vol. 10, no. 2, pp. 117–127, Apr. 2002.
- [11] Priyanka Thakur, Arshia Azam, “Edge Detection Through Integrated Morphological Gradient and Fuzzy Logic Approach”, *International Journal of Science, Engineering and Technology Research (IJSETR)*, Volume 4, Issue 5, May 2015, pp. 1613-1616.
- [12] F. Liu, “An efficient centroid type-reduction strategy for general type-2 fuzzy logic system,” *Information Sciences*, vol. 178, no. 9, pp. 2224–2236, May 2008.
- [13] J. Mendel, *Uncertain, Rule-Based Fuzzy Logic Systems: introduction and new directions*. Prentice-Hall, 2001.
- [14] N. N. Karnik, J. Mendel, and Q. Liang, “Type-2 fuzzy logic systems,” *IEEE Transactions on Fuzzy Systems*, vol. 7, no. 6, pp. 643–658, 1999.
- [15] L. A. Lucas, T. Centeno, and M. Delgado, “General type-2 fuzzy inference systems: analysis, design and computational aspects,” *IEEE International Conference on Fuzzy Systems*, London, UK, pp. 1107–1112, 2007.
- [16] J. M. Mendel, “On KM Algorithms for Solving Type-2 Fuzzy Set Problems,” vol. 21, no. 3, pp. 426–446, 2013.
- [17] D. Wu, “Approaches for Reducing the Computational Cost of Interval Type-2 Fuzzy Logic Systems: Overview and Comparisons,” *IEEE Transactions on Fuzzy Systems*, vol. 21, no. 1, pp. 80–99, Feb. 2013.
- [18] J. Mendel, *Uncertain, Rule-Based Fuzzy Logic Systems: introduction and new directions*. Prentice-Hall, 2001.
- [19] J. M. Mendel, “Comments on alpha-plane representation for type-2 fuzzy sets: theory and applications,” *IEEE Transactions on Fuzzy Systems*, vol. 18, no. 1, pp. 229–230, 2010.
- [20] R. C. Gonzalez, R. E. Woods and S. L. Eddins, *Digital Image Processing using Matlab*, Pearson Prentice Hall, 2004.
- [21] Priyanka Thakur, Arshia Azam, Mohd Haseeb Khan, “Morphological gradient based edge detection for image processing”, *National conference on circuits, signals and systems*. pp. 93 – 96, ISBN 978-93-82570-47-9, Jan 2015